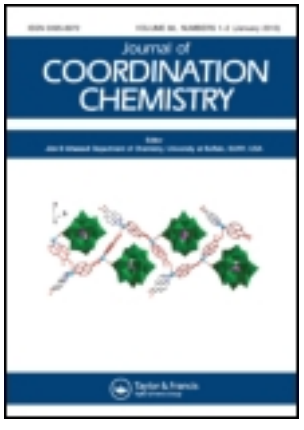

Journal of Coordination Chemistry
Publication details, including instructions for authors and subscription information:
http://www.tandfonline.com/loi/gcoo20

Diorganotin(IV) complexes with furan-2-carbohydrazone derivatives: synthesis, characterization, crystal structure and antibacterial activity

Tahereh Sedaghat [a], Leila Tahmasbi [a], Hossein Motamedi [b], Reyna Reyes-Martinez [c] & David Morales-Morales [c]

[a] Department of Chemistry, College of Sciences, Shahid Chamran University, Ahvaz, Iran

[b] Department of Biology, College of Sciences, Shahid Chamran University, Ahvaz, Iran

[c] Instituto de Química, Universidad Nacional Autónoma de México, Circuito Exterior s/n, Ciudad Universitaria, C.P. 04510, Mexico

Accepted author version posted online: 17 Jan 2013.

To cite this article: Tahereh Sedaghat , Leila Tahmasbi , Hossein Motamedi , Reyna Reyes-Martinez & David Morales-Morales (2013): Diorganotin(IV) complexes with furan-2-carbohydrazone derivatives: synthesis, characterization, crystal structure and antibacterial activity, Journal of Coordination Chemistry, 66:4, 712-724

To link to this article: http://dx.doi.org/10.1080/00958972.2013.767449

Journal of Coordination Chemistry
Vol. 66, No. 4, 20 February 2013, 712–724

Diorganotin(IV) complexes with furan-2-carbohydrazone derivatives: synthesis, characterization, crystal structure and antibacterial activity

TAHEREH SEDAGHAT*†, LEILA TAHMASBI†, HOSSEIN MOTAMEDI‡, REYNA REYES-MARTINEZ§ and DAVID MORALES-MORALES§

†Department of Chemistry, College of Sciences, Shahid Chamran University, Ahvaz, Iran
‡Department of Biology, College of Sciences, Shahid Chamran University, Ahvaz, Iran
§Instituto de Química, Universidad Nacional Autónoma de México, Circuito Exterior s/n, Ciudad Universitaria, C.P. 04510, México

(*Received 26 July 2012; in final form 13 November 2012*)

Four new diorganotin(IV) complexes, R_2SnL (L = L^a: R = Me **1**, Ph **2**; L = L^b: R = Me **3**, and Ph **4**), have been synthesized by reaction of hydrazone ONO donors, 5-bromo-2-hydroxybenzaldehyde furan-2-carbohydrazone (H_2L^a) and 2-hydroxynaphthaldehyde furan-2-carbohydrazone (H_2L^b) with diorganotin(IV) dichloride in the presence of a base. The compounds have been investigated by elemental analysis and IR, ^{1}H NMR, and ^{119}Sn NMR spectroscopies. Spectroscopic studies show that the hydrazone is a tridentate dianionic ligand, coordinating via the imine nitrogen and phenolic and enolic oxygens. The structures of H_2L^b and **3** have also been confirmed by X-ray crystallography. The results show that the structure of **3** is a distorted square pyramid with imine nitrogen in apical position. The *in vitro* antibacterial activities of ligands and complexes have been evaluated against gram-positive (*Bacillus cereus* and *Staphylococcus aureus*) and gram-negative (*Escherichia coli* and *Pseudomonas aeruginosa*) bacteria. H_2L^a and H_2L^b show no activity but the diphenyltin(IV) complexes exhibit good activities towards two bacterial strains in comparison with standard bacterial drugs.

Keywords: Organotin(IV); Hydrazone; Crystal structure; Antibacterial activity

1. Introduction

Research into organometallic compounds of tin(IV) is a prolific area of chemical investigations because these compounds have found more industrial, agricultural, and medicinal applications than any other organometallic compounds and present an interesting variety of structural possibilities [1–5]. The structure and coordination number of tin, the number and nature of the organic groups, and also the nature of donors attached to tin affect the properties, especially the bioactivity of organotin complexes [6,7], allowing properties to be tailored to a wide range of uses. In bioorganotin chemistry, an interesting area is introduction of bioactive ligands coordinated to the organotin fragment [8–11]. Schiff bases have received much attention due to their antibacterial and antitumor activities [12–14].

*Corresponding author. Email: tsedaghat@scu.ac.ir

Journal of Coordination Chemistry
ISSN 0095-8972 print/ISSN 1029-0389 online © 2013 Taylor & Francis
http://dx.doi.org/10.1080/00958972.2013.767449

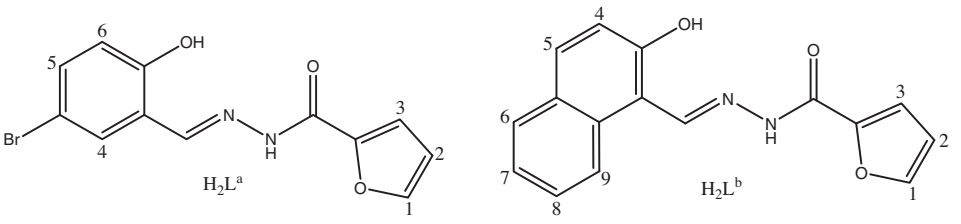

Figure 1. Structure of hydrazones with numbering for NMR assignments.

Hydrazones, as one kind of Schiff base, and their metal complexes, have potential pharmacological applications. Of interest structurally is the facile keto–enol tautomerization and availability of several potential donor sites allowing structural variety of their complexes [15]. Thus, hydrazone organotin(IV) complexes are of interest for both biological and structural reasons [16–19]. As part of our investigation dealing with organotin(IV) complexes of Schiff bases, this article presents the synthesis, structural studies, and antibacterial activities of four diorganotin(IV) complexes with two hydrazones, H_2L^a and H_2L^b (figure 1).

2. Experimental

2.1. *Materials and methods*

All starting materials were purchased from Merck except diphenyltin dichloride from Acros Company and were used as received. H_2L^a and H_2L^b have been reported earlier [20]. Herein, we have prepared these compounds by refluxing equimolar amounts of furan-2-carbohydrazide (2-furancarboxylic acid hydrazide) and 5-bromosalicylaldehyde or 2-hydroxynaphthaldehyde, respectively, in ethanol. All solvents were of reagent grade and used without purification. IR spectra were obtained using an FT BOMEM MB102 spectrophotometer. ^{1}H and ^{119}Sn NMR spectra were recorded with a Bruker 400 MHz Avance Ultrashield spectrometer.

2.2. *Synthesis of $SnMe_2L^a$ (1)*

Triethylamine (0.5 mmol) was added to a stirring solution of H_2L^a (0.077 g, 0.25 mmol) in methanol (5 mL). This solution was refluxed for 30 min. Then, a solution of Me_2SnCl_2 (0.055 g, 0.25 mmol) in methanol (3 mL) was added. The solution was refluxed for 2 h. After this, the yellow product was filtered and washed with methanol. Yield: 0.092 g (81%); m.p. 258 °C; Anal. Calcd for $C_{14}H_{13}BrN_2O_3Sn$: C, 36.87; H, 2.85; N, 6.14%. Found: C, 36.92; H, 2.82; N, 6.61%; FT-IR (KBr, cm^{-1}): ν(C=N), 1614; υ_{as}(Sn–C), 645; υ_s(Sn–C), 554; ν(Sn–O), 490; ν(Sn–N), 459; ^{1}H NMR (DMSO-d$_6$): $\delta = 0.87$ [s, 6H, $SnMe_2$, $^2J(^{119}Sn–^1H) = 78.4$ Hz], 6.53 (m, 1H, H_2), 6.67 (d, 1H, H_6, $J_{HH} = 8.9$ Hz), 7.08 (d, 1H, H_3, $J_{HH} = 3.4$ Hz), 7.25 (d, 1H, H_4, $J_{HH} = 2.4$ Hz), 7.38 (dd, 1H, H_5, $J_{HH} = 8.9$, 2.4 Hz), 7.57 (d, 1H, H_1, $J_{HH} = 0.6$ Hz), 8.66 [s, 1H, HC=N, $^3J(^{119}Sn-^1H) = 44.1$ Hz]; and ^{119}Sn NMR ($CDCl_3$): $\delta = -152$.

2.3. *Synthesis of [$SnPh_2L^a$]·CH_3OH (2)*

Complex **2** was synthesized as described for **1** from Ph_2SnCl_2 (0.086 g, 0.25 mmol). Yield: 0.119 g (82.6%); m.p. 218 °C; Anal. Calcd for $C_{25}H_{21}BrN_2O_4Sn$: C, 49.05; H, 3.43; N, 4.57%. Found: C, 48.92; H, 2.86; N, 5.04%; FT-IR (KBr, cm^{-1}): ν(C=N), 1610; ν(Sn–O), 496; ν(Sn–N), 449; ^{1}H NMR (DMSO-d_6): $\delta = 6.66$ (m, 1H, H_2), 6.84 (d, 1H, H_6, $J_{HH} = 8.8$ Hz), 7.15 (d, 1H, H_3, $J_{HH} = 3.6$ Hz), 7.29–7.36 [m, 6H, $H_{m,p}$ (Ph_2Sn)], 7.41 (dd, 1H, H_5, $J_{HH} = 8.9$, 2.6 Hz), 7.56 [dd, 4H, H_o(Ph_2Sn), $J_{HH} = 7.7$, 1.7 Hz)], 7.62 (d, 1H, H_4, $J_{HH} = 2.6$ Hz), 7.87 (d, 1H, H_1, $J_{HH} = 0.6$ Hz), 8.68 [s, 1H, HC=N]; and ^{119}Sn NMR ($CDCl_3$): $\delta = -325.2$.

2.4. *Synthesis of $SnMe_2L^b$ (3)*

H_2L^b (0.070 g, 0.25 mmol) was dissolved in methanol (10 mL) and KOH (0.028 g, 0.5 mmol) was added. The solution was refluxed for 30 min and then, $SnMe_2Cl_2$ (0.055 g, 0.25 mmol) in methanol (3 mL) was added dropwise. This yellow solution was refluxed for 2 h and after cooling, KCl was centrifuged. Orange rectangular crystals were formed after several days at room temperature. These crystals were used for crystallography. Yield: 0.049 g (46.2%); m.p. 150 °C; Anal. Calcd for $C_{18}H_{16}N_2O_3Sn$: C, 50.61; H, 3.74; N, 6.56%. Found: C, 50.64; H, 3.81; N, 6.32%; FT-IR (KBr, cm^{-1}): ν(C=N), 1618; υ_{as}(Sn–C), 630; υ_s(Sn–C), 566; ν(Sn–O), 508; ν(Sn–N), 468; ^{1}H NMR (DMSO-d_6): $\delta = 0.70$ [s, 6H, $SnMe_2$, $^2J(^{119}Sn–^1H) = 88.3$ Hz], 6.63 (dd, 1H, H_2, $J_{HH} = 3.4$, 1.8 Hz), 6.92 (d, 1H, H_4, $J_{HH} = 9.0$ Hz), 7.03 (dd, 1H, H_3, $J_{HH} = 3.6$, 0.7 Hz), 7.30 (t, 1H, H_7, $J_{HH} = 7.5$ Hz), 7.50 (t, 1H, H_8, $J_{HH} = 8.4$ Hz), 7.77 (dd, 1H, H_6, $J_{HH} = 7.9$, 1.0 Hz), 7.84 (dd, 1H, H_1, $J_{HH} = 1.8$, 0.8 Hz), 7.86 (d, 1H, H_5, $J_{HH} = 9.0$ Hz), 8.23 (d, 1H, H_9, $J_{HH} = 8.5$ Hz), 9.51 [s, 1H, HC=N, $^3J(^{119}Sn–^1H) = 36.5$ Hz]; and ^{119}Sn NMR (DMSO): $\delta = -227.4$.

2.5. *Synthesis of [$SnPh_2L^b$]·CH_3OH (4)*

Complex **4** was synthesized as described for **2** from H_2L^b (0.070 g, 0.25 mmol). The product was obtained as orange powder. Yield: 0.095 g (69.3%); m.p. 172 °C; Anal. Calcd for $C_{29}H_{24}N_2O_4Sn$: C, 59.98; H, 4.11; N, 4.80%. Found: C, 59.94; H, 3.58; N, 5.26%; FT-IR (KBr, cm^{-1}): ν(C=N), 1618; ν(Sn–O), 512; ν(Sn–N), 450. ^{1}H NMR (DMSO-d_6): $\delta = 6.67$ (m, 1H, H_2), 7.15–7.18 (m, 2H, $H_{3,4}$), 7.30–7.40 [m, 7H, $H_{m,p}$ (Ph_2Sn), H_7], 7.50 (t, 1H, H_8, $J_{HH} = 7.6$ Hz), 7.65 [dd, 4H, H_o(Ph_2Sn), $J_{HH} = 6.7$, 1.0 Hz)], 7.80 (d, 1H, H_6, $J_{HH} = 7.9$ Hz), 7.89–7.93 (t, 2H, $H_{1,5}$), 8.26 (d, 1H, H_9, $J_{HH} = 8.6$ Hz), 9.55 [s, 1H, HC=N, $^3J(^{119}Sn–^1H) = 52.8$ Hz]; and ^{119}Sn NMR ($CDCl_3$): $\delta = -328.1$.

2.6. *X-ray crystal structure determination*

Crystalline green-yellow prisms of H_2L^b and **3** were grown by slow evaporation from saturated solutions of ethanol and methanol, respectively, and mounted in random orientation on glass fibers. In all cases, the X-ray intensity data were measured at 298 K on a Bruker SMART APEX CCD-based three-circle X-ray diffractometer system using graphite monochromated Mo-Kα ($\lambda = 0.71073$ Å) radiation. The detector was placed 4.837 cm from the crystals in all cases. A total of 1800 frames were collected with a scan width of 0.3° in ω and an exposure time of 10 s/frame. The frames were integrated with the Bruker SAINT software package [21a] using a narrow-frame integration algorithm. The integration of the

Table 1. Crystallographic and structure refinement data for $H_2L^b \cdot H_2O$ and **3**.

	$H_2L^b \cdot H_2O$	**3**
Empirical formula	$C_{16}H_{14}N_2O_4$	$C_{18}H_{16}N_2O_3Sn$
Formula weight	298.29	427.02
T (K)	298(2)	298(2)
Wavelength, λ (Å)	0.71073	0.71073
Crystal system	Monoclinic	Monoclinic
Space group	$P2_1/n$	$P2_1/c$
Crystal size (mm^3)	$0.36 \times 0.13 \times 0.05$	$0.30 \times 0.18 \times 0.04$
a (Å)	4.5423(7)	12.850(11)
b (Å)	23.985(4)	17.062(15)
c (Å)	13.361(2)	7.645(7)
β (°)	95.179(3)	94.506(15)
V ($Å^3$)	1449.7(4)	1671(2)
Z	4	4
$D_{calc.}$ ($mg\,m^{-3}$)	1.367	1.698
θ Ranges for data collection (°)	1.70–25.39	1.59–25.61
$F(000)$	624	848
Absorption coefficient (mm^{-1})	0.100	1.547
Index ranges	$-5 \leqslant h \leqslant 5$ $-28 \leqslant k \leqslant 28$ $-16 \leqslant l \leqslant 16$	$-15 \leqslant h \leqslant 15$ $-20 \leqslant k \leqslant 20$ $-9 \leqslant l \leqslant 9$
Reflections collected	11,988	13,800
Independent reflections	2679 [R(int) = 0.0589]	3104 [R(int) = 0.0767]
Max. and min. transmission	0.8620 and 0.7636	0.9408 and 0.6317
Data/restraints/parameters	2679/4/211	3104/0/219
Goodness-of-fit on F^2	1.010	0.848
Final R indices [$I > 2\sigma(I)$]	$R1 = 0.0551$ $wR_2 = 0.1081$	$R_1 = 0.0341$ $wR_2 = 0.0568$
R indices (all data)	$R_1 = 0.1154$ $wR_2 = 0.1318$	$R_1 = 0.0585$ $wR_2 = 0.0619$
Largest diff. peak and hole ($e.A^{-3}$)	0.153 and −0.147	0.534 and −0.387

data was done using monoclinic unit cells in both cases to yield a total of 11988 (H_2L^b) and 13800 (**3**) reflections, respectively, to a maximum 2θ angle of 50.00° (0.93 Å resolution) for both compounds, of which 2679 (H_2L^b) and 3104 (**3**) were independent. Analysis of the data showed, in all cases, negligible decays during data collection. The structures were solved by Patterson method using SHELXS-97 [21b]. The remaining atoms were located via a few cycles of least squares refinements and difference Fourier maps using $P2_1/n$ or $P2_1/c$ space groups for H_2L^b and **3**, respectively, with $Z = 4$ in both cases. Hydrogen atoms were input at calculated positions and allowed to ride on the atoms to which they are attached. Thermal parameters were refined for hydrogen atoms on the phenyl groups with $U_{iso}(H) = 1.2\ U_{eq}$ of the parent in all cases. The final cycle of refinement was carried out on all nonzero data using SHELXL-97 [21c] and anisotropic thermal parameters for all nonhydrogen atoms. The details of the structure determinations are given in table 1.

2.7. *Antibacterial tests*

The *in vitro* antibacterial activities of ligands and organotin(IV) complexes were investigated against standard strains of two gram-positive, (*Bacillus cereus* and *Staphylococcus*

aureus ATCC 6538), and two gram-negative, (*Escherichia coli* ATCC 11303 and *Pseudomonas aeruginosa* ATCC 27853), bacteria. In order to compare the results, Vancomycin (30 mg/disk), Streptomycin (10 mg/disk), penicillin (10 mg/disk), Nalidixic acid (30 mg/disk), and Gentamicin (10 mg/disk) were used as standard antibacterial drugs. Determination of the antibacterial activity was carried out by paper disk diffusion. The compounds were dissolved in dimethyl sulfoxide (DMSO) at 5, 10, 20, and 40 mg mL^{-1} concentration. Muller Hinton broth was used for preparing basal media for the bioassay of the organisms. A lawn culture from 0.5 MacFarland suspension of each strain was prepared on Muller Hinton agar. Blank paper disks (6.4 mm diameter) were saturated with a solution of test compounds (40 μL) and placed on the surface of the agar plates. On one paper disk, only DMSO was poured as a control. The plates were incubated at 37 °C for 24 h and the inhibition zone diameters around each disk was measured in mm.

3. Results and discussion

Hydrazones, H_2L^a and H_2L^b, were synthesized by condensation of furan-2-carbohydrazide with 5-bromo-2-hydroxybenzaldehyde and 2-hydroxynaphthaldehyde, respectively. Owing to the existence of ketoamide group (NH–C=O) in the structure, two tautomerizations, keto–amine and enol–imine, are possible. Aldimine Schiff bases may exhibit tautomerism between the phenol–imine and the keto–amine forms, so two tautomers are also predicted for aldehyde of these molecules. figure 2 shows these possible tautomeric equilibria for H_2L^b. On the basis of an earlier report [20a], H_2L^a is in tautomeric form I in the solid state. Herein, we report the crystal structure and nature of the intramolecular hydrogen bonds for H_2L^b.

Complexes **1**–**4** were prepared by reaction of R_2SnCl_2 (R = Me and Ph) with corresponding hydrazone in methanol in the presence of a base to force deprotonation of the ligand. The new complexes were characterized by elemental analysis and IR and NMR spectroscopy. The structure of $SnMe_2L^b$ has also been determined by X-ray diffraction.

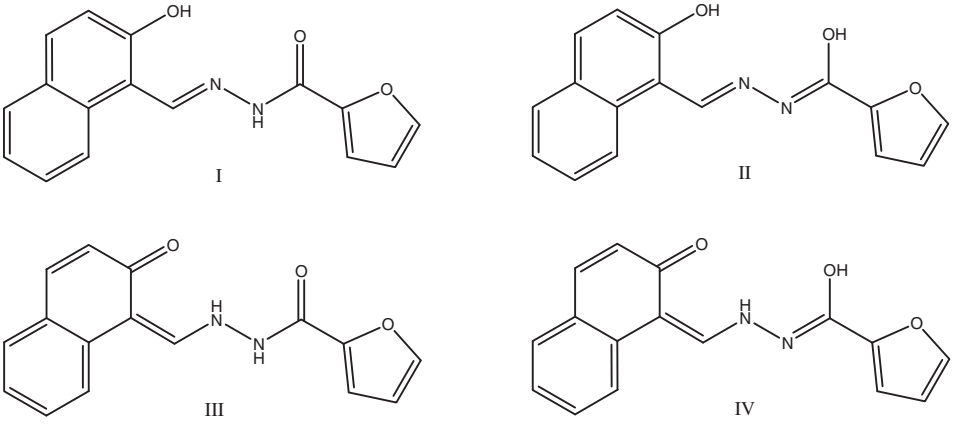

Figure 2. Tautomeric forms for H_2L^b.

3.1. *Spectroscopic studies*

In IR spectra of complexes, the disappearance of ν_{O-H} and ν_{N-H} shows complete deprotonation of ligand and its subsequent coordination to tin. The absence of $\nu_{C=O}$ in complexes confirms that the ligand coordinates with tin in the enol form [22]. The $\nu_{C=N}$ of ligands (1620–1625 cm^{-1}) shifts to lower wavenumber in complexes. This observation indicates that the imine nitrogen is involved in coordination to tin. The appearance of new bands in IR spectra of the complexes assigned to ν(Sn–N) and ν(Sn–O) supports bonding of nitrogen and oxygen to tin [23–26]. Presence of both ν_s(Sn–C) and ν_{as}(Sn–C) in **1** and **3** is consistent with a nonlinear Me–Sn–Me configuration.

In ^{1}H NMR spectra of ligands, the CH=N proton is a singlet, supporting the location of hydrogen on oxygen and, therefore, no HCNH coupling, indicating phenol–imine form in solution (I or II, figure 2). The signal at 11.16 and 12.25 ppm in H_2L^a and H_2L^b, respectively, may be attributed to –NHN = in tautomeric form I. In ^{1}H NMR spectra of the complexes, absence of signals due to acidic hydrogen atoms suggests deprotonation of ligand and coordination to tin in the enol form. In ^{1}H NMR spectra of complexes satellites around azomethine proton signal, the $^3J(^{119}Sn–^1H)$ coupling indicates the ligation of azomethine nitrogen.

^{1}H NMR spectra of **1** and **3** show a singlet for $SnMe_2$ accompanied by satellites with $^2J(^{119}Sn–^1H)$ larger than uncomplexed $SnMe_2Cl_2$ (68.7 Hz). Generally, the larger coupling constant indicates higher coordination number of tin [4]. Substitution of $^2J(^{119}Sn–^1H)$ in the Lockhart–Manders equation [27] gives a value of 128.87° and 142.37° for Me–Sn–Me angle in **1** and **3**, respectively. The ^{1}H NMR spectra of diphenyltin complexes show a multiplet attributable to the $H_{m,p}$ of Ph_2Sn moiety. This signal has ^{119}Sn satellites due to $^1H–^{119}Sn$ coupling, but $^3J(^{119}Sn–^1H)$ value cannot be extracted from the spectrum.

$^{119}Sn\{^1H\}$NMR spectra of all complexes show one sharp singlet at significantly lower frequency than that of the original $SnMe_2Cl_2$ (+137 ppm) and $SnPh_2Cl_2$ (−32 ppm) [4]. This large upfield shift is because of increasing coordination number of tin. On the basis of the chemical shifts observed for phenyltin and methyltin derivatives [25,26,28–30], the coordination number of tin is five for **1**–**4**.

3.2. *X-ray structures of $H_2L^b·H_2O$ and $[SnMe_2L^b]$*

The molecular structure of H_2L^b is shown in figure 3. This compound crystallizes as the monohydrate. Selected bond lengths and angles are listed in table 2. The orthorhombic unit cell contains four molecules. The crystal structure is stabilized by hydrogen bonding between the crystallization water and adjacent hydrazone. There is also a hydrogen bond between oxygen of water and hydrazinic NH of one molecule and another between the two hydrogen atoms of water with two amide oxygen atoms of two other molecules in the lattice. Therefore, one water molecule participates in three different hydrogen bonds with three hydrazone molecules and also each amide oxygen forms two hydrogen bonds with two water molecules. H_2L^b shows a *trans*-C=N–N–C conformation with intramolecular hydrogen bonding from phenolic OH to azomethine nitrogen [O2–H2, 0.853 Å; H2···N2, 1.802 Å; O2–H···N2, 150.61°]. According to the crystal structure, H_2L^b is in the keto–amine tautomeric form in hydrazine and in phenol–imine form in the aldehyde (form I, figure 2 *vide supra*).

Figure 4 shows the molecular structure with atomic numbering scheme for $SnMe_2L^b$. Selected bond distances and angles are given in table 3. Complex **3** crystallizes in the

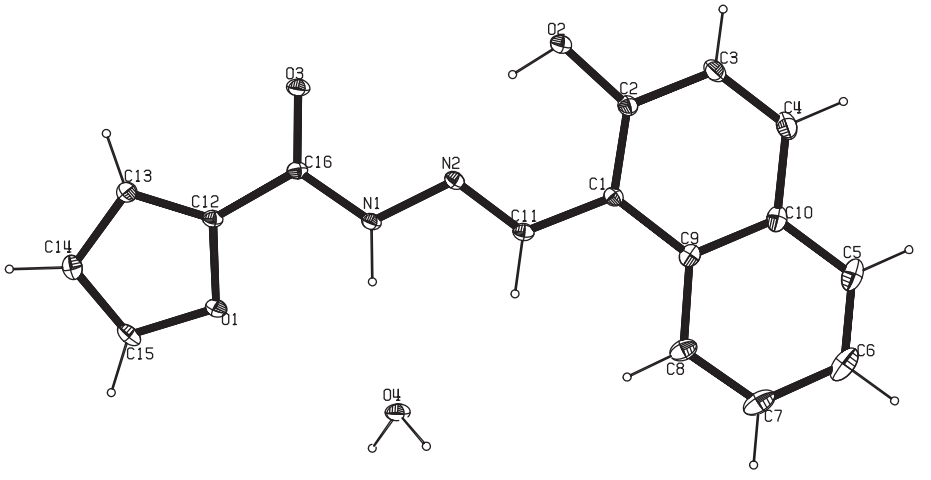

Figure 3. Crystal structure of $H_2L^b \cdot H_2O$.

Table 2. Selected bond lengths (Å) and angles (°) for $H_2L^b \cdot H_2O$.

N(1)–C(16)	1.338(3)
N(1)–N(2)	1.380(3)
N(1)–H(1)	0.898(10)
N(2)–C(11)	1.282(3
O(1)–C(15)	1.362(3)
O(1)–C(12)	1.362(3)
O(2)–C(2)	1.353(3)
O(2)–H(2)	0.853(10)
O(3)–C(16)	1.234(3)
O(4)–H(4A)	0.852(10)
O(4)–H(4B)	0.850(10)
C(1)–C(11)	1.438(3)
C(12)–C(16)	1.453(4)
C(16)–N(1)–N(2)	118.8(2)
C(16)–N(1)–H(1)	125.5(16)
N(2)–N(1)–H(1)	115.6(16)
C(11)–N(2)–N(1)	116.5(2)
C(2)–O(2)–H(2)	105(2)
H(4A)–O(4)–H(4B)	105(3)
O(3)–C(16)–N(1)	123.9(2)
O(3)–C(16)–C(12)	120.6(3)
N(1)–C(16)–C(12)	115.5(2)

monoclinic space group $P2_1/c$. The hydrazone is a tridentate dibasic ligand coordinated via nitrogen from the imine and the two oxygens from the phenolate and enolate. The coordination sphere is completed by two methyls coordinated sigma through carbon. Therefore, the tin is of five coordinates and the furan oxygen has no coordination to tin; thus, the ligand forms six- and five-membered chelate rings. To quantify the extent of the distortion from either the ideal square pyramid (SP) or trigonal bipyramid (TBP), the index of trigonality, τ, defined by Reedijk and coworkers [31], has been determined. The τ value is 0.15 for $SnMe_2L^b$ and, thus, the metal coordination geometry is better described as distorted SP ($\tau = 0.0$ and 1.0 for SP or TBP geometries, respectively) with the imine nitrogen

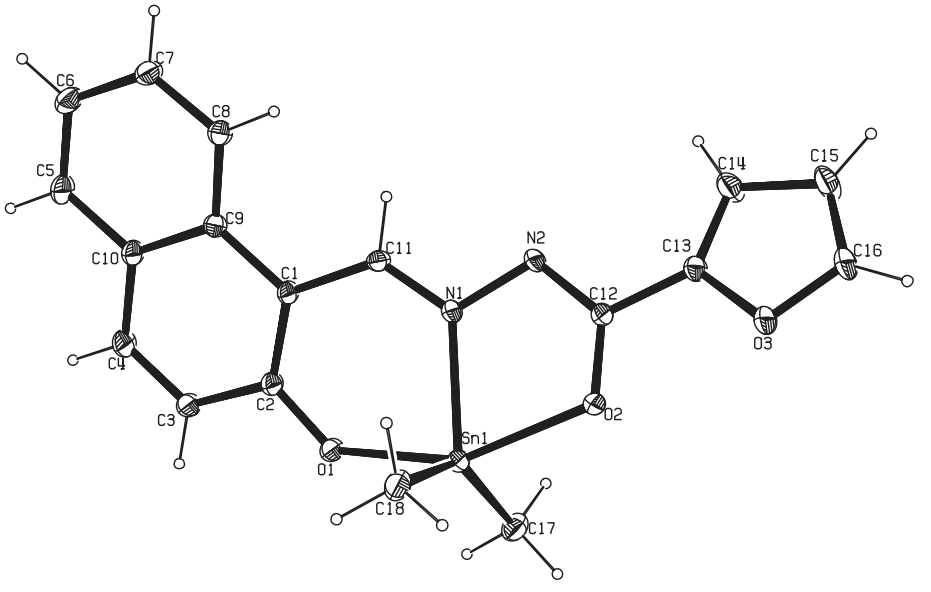

Figure 4. Crystal structure of $SnMe_2L^b$.

occupying the apical position. N1 is chosen as apex because the four donors that define the two largest angles around the metal atom should not be in the axial position [31]. The O1–Sn–O2 and C17–Sn–C18 bond angles (142.97 and 152.03, respectively) deviate from 180° and the O1–Sn–N1, O2–Sn–N1, C17–Sn–N1, and C18–Sn–N1 angles (80.82, 72.46°, 113.99°, and 103.04°, respectively) deviate from the 90° angle expected for a perfect SP. This distortion is mainly due to the rigidity of the chelate rings and is facilitated by the large covalent radius of Sn(IV) [32,33]. An empirical estimation of the C–Sn–C angle in solution (142.37° is in reasonable agreement with the angle observed in the solid state (142.97°). The increasing C–O and decreasing C–N bond lengths in the amide upon complexation indicates enolization and charge delocalization in the hydrazinic upon deprotonation and coordination. Therefore, C–O goes from a carbonyl in the ligand to an enolate in the complex and C–N from a single bond to a double bond in the complex. The values of these bond lengths in the complex (1.287 and 1.292 Å, respectively) are consistent with the enolate form of the amide [23,34]. The lengthening of the C–N(imine) from 1.282(3) Å in the free ligand to 1.291(4) Å coordinated to the metal (C11–N1) is a consequence of the involvement of the nitrogen of the imine in coordination. The Sn–N1, Sn–O1, and Sn–O2 bond lengths are 2.148(3), 2.105(3), and 2.158(3) Å, respectively, similar to the sum of the covalent radii of Sn–N (2.15 Å) and Sn–O (2.10 Å), indicating covalent bond of tin with both oxygen and imine nitrogen. The Sn–O(phenolate) bond is shorter than Sn–O(enolate). The molecules arrange as centrosymmetric dimers generated by intermolecular secondary Sn···O2 [2.987(4)å] interactions generating a Sn_2O_2 four-membered ring [figure 5(a)]. The Sn···O interaction distance (2.987 Å) is much longer than the sum of the covalent radii of the tin and oxygen atoms (2.10 Å), but significantly shorter than the sum of the van der Waal's radii (3.68 Å) [35,36]. The Sn–O···Sn–O torsion angle is zero and shows evidence of coplanarity. The secondary Sn···O interaction also modifies the geometry of tin, occupying the apical position in the distorted SP having angles between 64° and 142° (table 3). Similar to most Schiff base–tin complexes reported, the

Table 3. Selected bond lengths (Å) and angles (°) for **3**.

Sn(1)–C(17)	2.073(4)
Sn(1)–C(18)	2.100(4)
Sn(1)–O(1)	2.105(3)
Sn(1)–N(1)	2.148(3)
Sn(1)–O(2)	2.158(3)
O(1)–C(2)	1.302(4)
O(2)–C(12)	1.287(4)
N(1)–C(11)	1.291(4)
N(1)–N(2)	1.398(4)
N(2)–C(12)	1.292(5)
C(1)–C(11)	1.421(5)
C(12)–C(13)	1.462(5)
Sn(1)···O(2)	2.987(4)
C(17)–Sn(1)–C(18)	142.97(17)
C(17)–Sn(1)–O(1)	89.95(14)
C(18)–Sn(1)–O(1)	96.34(14)
C(17)–Sn(1)–N(1)	113.99(16)
O(1)–Sn(1)–N(1)	80.82(10)
C(17)–Sn(1)–O(2)	93.40(14)
C(18)–Sn(1)–O(2)	97.54(15)
O(1)–Sn(1)–O(2)	152.03(11)
N(1)–Sn(1)–O(2)	72.46(10)
C(2)–O(1)–Sn(1)	132.1(2)
C(12)–O(2)–Sn(1)	113.5(2)
C(11)–N(1)–Sn(1)	127.7(3)
N(2)–N(1)–Sn(1)	117.2(2)
C(12)–N(2)–N(1)	110.3(3)
C(2)–C(1)–C(11)	121.6(4)
O(1)–C(2)–C(1)	123.8(3)
N(1)–C(11)–C(1)	127.2(4)
O(2)–C(12)–N(2)	125.8(3)
O(1)–Sn–O(2)	142.37(9)
C(17)–Sn–O(2)	75.48(11)
C(18)–Sn–O(2)	77.51(11)
O(2)–Sn–O(2)	64.80(8)
N(1)–Sn–O(2)	136.81(9)

O–Sn interaction occurs with the oxygen that forms part of the five-membered chelate ring, attributed to the increased "*s*" character [28,37,38]. In the absence of both amine and hydroxyl groups, the interactions that stabilize the crystal arrangement are weak hydrogen bonds (C–H···N, C–H···N) and π–π interactions. Both C–H···N and π–π interactions generate a linear arrangement along the *c* axis; the π–π interactions between aromatic rings have distances of 3.978 and 3.870 Å centroid–centroid [figure 5(b)].

3.3. *Antibacterial studies*

The *in vitro* antibacterial activities of the Schiff bases and their organotin(IV) complexes were studied along with five standard antibacterial drugs *viz*, Vancomycin, Streptomycin, penicillin, Nalidixic acid, and Gentamycin. The micro-organisms used in this work include *B. cereus* and *S. aureus* (as gram-positive bacteria) and *E. coli* and *P. aeruginosa* (as gram-negative bacteria). The results are presented in table 4. Comparing the biological activity of the ligands, organotin(IV) complexes and standard drugs, H_2L^a and H_2L^b have no activity, **1** and **3** have low activity towards all bacterial strains and **2** and **4** exhibit good

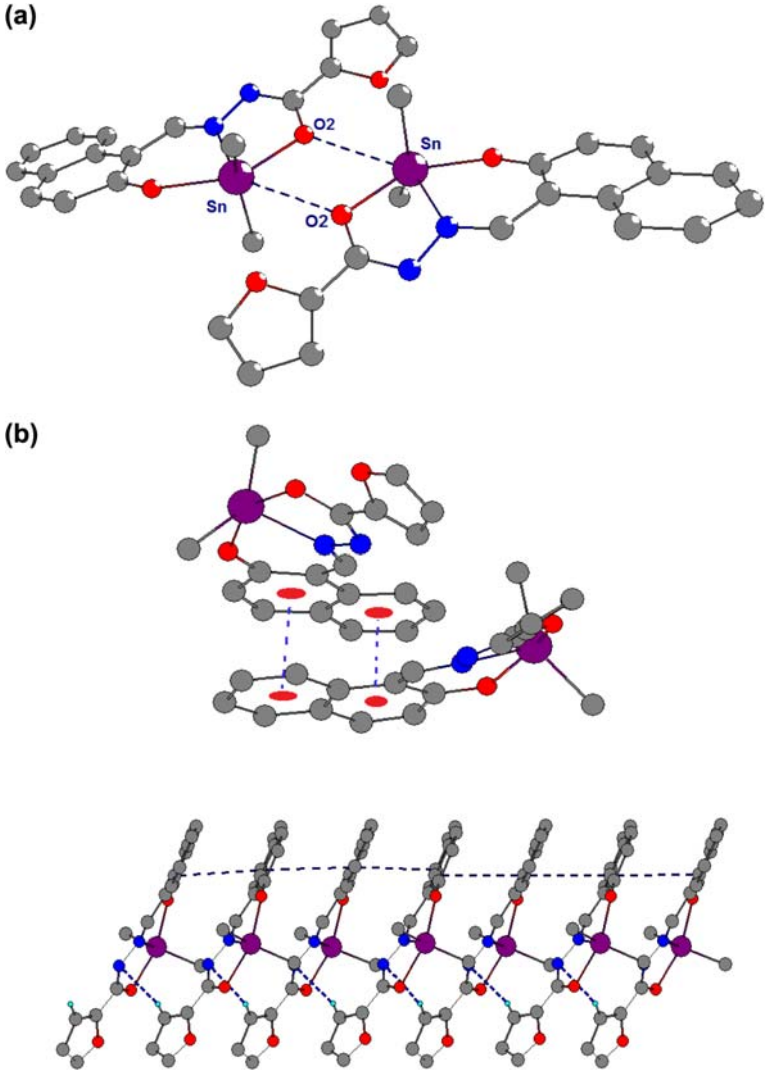

Figure 5. (a) Centrosymmetric dimers generated by secondary Sn···O_2 interactions in $SnMe_2L^b$; (b) aromatic $\pi\cdots\pi$ interactions in $SnMe_2L^b$. Hydrogen atoms were omitted for clarity.

inhibitory effects towards two bacterial strains. In general, the enhancement in activity of the ligand on complexation with organotins may be due to increasing the lipophilic character and efficient diffusion of the metal complexes into bacterial cell (chelation theory) [39–42] and also because of the intrinsic biological activity effects of organotin moiety. The diphenyltin complexes show more inhibition on microbial growth than dimethyltin complexes. The presence of two phenyl groups increases the solubility in lipids and they can cross through the cell walls with higher efficiency [43]. Generally, biological activity of organotin complexes is influenced both by donor ligand and by the number and nature of the organic groups bound to tin. Since permeability across the bacterial cell wall is necessary for the effectiveness of the biocide compounds, therefore, lipophilicity is an important

Table 4. Antibacterial activities of ligands and their organotin(IV) complexes.

Compound	Conc. (mg mL^{-1})	Inhibition zone (mm)			
		E. coli	*P. aeruginosa*	*S. aureus*	*B. cereus*
H_2L^a	40	n.a.	n.a.	n.a.	n.a.
H_2L^b	40	n.a.	11	n.a.	n.a.
$SnMe_2L^a$ (**1**)	20	12	n.a.	11	n.a.
	40	12	n.a.	11	n.a.
$SnPh_2L^a$ (**2**)	5	15	12*	16	12
	10	16	12*	17	12
	20	17	12*	18	12
	40	18	12*	18	12
$SnMe_2L^b$ (**3**)	20	14	12	12	14
	40	14	14	13	16
$SnPh_2L^b$ (**4**)	5	16	9*	18	12
	10	16	10*	18	12
	20	17	12*	19	12
	40	19	13*	20	14
Vancomycin		22	8	16	15
Streptomycin		11	11	11	18
Penicillin		16	n.a.	17	n.a.
Nalidixic acid		28	10	11	17
Gentamicin		21	19	17	20

Note: *Pigment production inhibition, n.a. = no activity.

factor making the drug more soluble in lipids which facilitate microorganism membrane crossing. Complex **4** is most active compound and this activity may also be attributed to lipophilicity which increased due to presence of the naphthalene ring. Since **2** and **4** show only pigment production inhibition against *P. aeruginosa*, it may be postulated that these compounds inhibit part of the metabolic pathways of this organism.

4. Conclusions

Hydrazone ligands are completely deprotonated and coordinate tridentate to tin via imine nitrogen and phenolic and enolic oxygens. On the basis of ^{119}Sn NMR data, coordination number of tin remains five in solution. Since most research for new antitumor drugs depend on antibiotics affecting gram-negative bacteria [44], it is probable that these new organotin(IV) complexes have antitumor effects. Diorganotin(IV) complexes generally exhibit higher antitumor activity than other tin derivatives and within the diorganotin(IV) class, the highest activity together with lowest toxic effect is shown by diphenyl-tin(IV) complexes [6,45–47]. Therefore, it is suggested that **2** and **4** may be good candidates for cytotoxicity studies.

Supplementary material

CCDC 863731 and 863732 contain the supplementary crystallographic data for H_2L^b and **3**, respectively. These data can be obtained free of charge via http://www.ccdc.cam.ac.uk/conts/retrieving.html, or from the Cambridge Crystallographic Data Center, 12 Union Road, Cambridge CB2 1EZ, UK; Fax: (+44) 1223-336-033; or email: deposit@ccdc.cam.ac.uk.

Acknowledgments

Support of this work by Shahid Chamran University, Ahvaz, Iran (Grant 1391) is gratefully acknowledged. DMM would like to thank generous support by CONACYT (F58692) and DGAPA-UNAM (IN227008). RRM thanks CONACYT for a postdoctoral scholarship (Agreement No. 290586-UNAM).

References

[1] M. Gielen, E.R.T. Tiekink. In *Metallotherapeutic Drugs and Metal-based Diagnostic Agents*, M. Gielen, E.R.T. Tiekink (Eds.), Chap. 22, Wiley, Chichester (2005).
[2] P.J. Smith (Ed.). *Chemistry of Tin*, Blackie, London (1998).
[3] A.G. Davies, M. Gielen, K.H. Pannell, E.R.T. Tiekink (Eds.). *Tin Chemistry: Fundamentals, Frontiers, and Applications*, Wiley, Chichester (2008).
[4] A.G. Davies. *Organotin Chemistry*, 2nd Edn. Edn, Wiley-VCH, Weinheim (2004).
[5] A. Tarassoli, T. Sedaghat. In *Organometallic Chemistry Research Perspectives*, R.P. Irwin (Ed.), Chap. 7, Nova, New York, NY (2007).
[6] C. Pellerito, L. Nagy, L. Pellerito, A. Szorcsik. *J. Organomet. Chem.*, **691**, 1733 (2006).
[7] X. Song, A. Zapata, G. Eng. *J. Organomet. Chem.*, **691**, 1756 (2006).
[8] L. Pellerito, L. Nagy. *Coord. Chem. Rev.*, **224**, 111 (2002).
[9] M. Nath, S. Pokharia, R. Yadav. *Coord. Chem. Rev.*, **215**, 99 (2001).
[10] E. Katsoulakou, M. Tiliakos, G. Papaefstathiou, A. Terzis, C. Raptopoulou, G. Geromichalos, K. Papazisis, R. Papi, A. Pantazaki, D. Kyriakidis, P. Cordopatis, E.M. Zoupa. *J. Inorg. Biochem.*, **102**, 1397 (2008).
[11] M. Nath, S. Pokharia, X. Song, G. Eng, M. Gielen, M. Kemmer, M. Biesemans, R. Willem, D. Vos. *Appl. Organomet. Chem.*, **17**, 305 (2003).
[12] M. Sönmez, M. Çelebi, İ. Berber. *Eur. J. Med. Chem.*, **45**, 1935 (2010).
[13] H.F.A. El-halim, M.M. Omar, G.G. Mohamed. *Spectrochim. Acta, Part A*, **78**, 36 (2011).
[14] G.G. Mohamed, M.A. Zayed, S.M. Abdallah. *J. Mol. Struct.*, **979**, 62 (2010).
[15] A.M. Stadler, J. Harrowfield. *Inorg. Chim. Acta*, **362**, 4298 (2009).
[16] E.L. Torres, F. Zani, M.A. Mendiola. *J. Inorg. Biochem.*, **105**, 600 (2011).
[17] M.A. Affan, S.W. Foo, I. Jusoh, S. Hanapi, E.R.T. Tiekink. *Inorg. Chim. Acta*, **362**, 5031 (2009).
[18] M. Hong, H.D. Yin, S.W. Chen, D. Wang. *J. Organomet. Chem.*, **695**, 653 (2010).
[19] H. Yin, J. Li, M. Hong, J. Cui, L. Dong, Q. Zhang. *J. Mol. Struct.*, **985**, 261 (2011).
[20] (a) X.S. Tai, L. Yin, M.Y. Hao, Z.P. Liang. Acta Cryst., **E63**, o2144 (2007); (b) P. Melnyk, V. Leroux, C. Sergheraert, P. Grellier. *Bioorg. Med. Chem. Lett*., **16**, 31 (2006); (c) K.B. Gudasi, T.R. Goudar. *Polish J. Chem*., **73**, 385 (1999).
[21] (a) Bruker AXS, *SAINT Software Reference Manual*, Madison, WI (1998); (b) G.M. Sheldrick. *Acta Crystallogr., Sect. A*, **46**, 467 (1990); (c) G.M. Sheldrick, SHELXL-97, *Program for Crystal Structure Refinement*, University of Göttingen, Germany (1998).
[22] H.D. Yin, J.C. Cui, Y.L. Qiao. *Polyhedron*, **27**, 2157 (2008).
[23] T. Sedaghat, Z. Shokohi-pour. *J. Coord. Chem.*, **62**, 3837 (2009).
[24] B. Yearwood, S. Parkin, D.A. Atwood. *Inorg. Chim. Acta*, **333**, 124 (2002).
[25] T. Sedaghat, M. Monajjemzadeh, H. Motamedi. *J. Coord. Chem.*, **64**, 3169 (2011).
[26] T. Sedaghat, M. Naseh, H.R. Khavasi, H. Motamedi. *Polyhedron*, **33**, 435 (2012).
[27] T.P. Lockhart, W.F. Manders. *Inorg. Chem.*, **25**, 892 (1986).
[28] V. Barba, E. Vega, R. Luna, H. Hopfl, H.I. Beltran, L.S. Zamudio-Rivera. *J. Organomet. Chem.*, **692**, 731 (2007).
[29] J. Otera. *J. Organomet. Chem.*, **221**, 57 (1981).
[30] D. Kovala-Demertzi, P. Tauridou, U. Russo, M. Gielen. *Inorg. Chim. Acta*, **239**, 177 (1995).
[31] A.W. Addison, T.N. Rao, J. Reedijk, J. van Rijn, G.C. Verschoor. *J. Chem. Soc., Dalton Trans*., 1349 (1984).
[32] S.G. Öztas, E. Sahin, N. AncIn, S. Ide, M. Tüzün. *J. Mol. Struct.*, **705**, 107 (2004).
[33] C. Pettinari, F. Marchetti, R. Pettinari, D. Martini, A. Drozdov, S. Troyanov. *Inorg. Chim. Acta*, **325**, 103 (2001).
[34] H.D. Yin, M. Hong, G. Li, D.Q. Wang. *J. Organomet. Chem.*, **690**, 3714 (2005).
[35] M.A. Affan, M.A. Salam, F.B. Ahmad, J. Ismail, M.B. Shamsuddin, H.M. Ali. *Inorg. Chim. Acta*, **366**, 227 (2011).
[36] L.N. Sun, C.W. Hu. Acta Cryst., Sect. E, **63**, m1832 (2007).

[37] L.S. Zamudio-Rivera, R. George-Tellez, G. Lopez-Mendoza, A. Morales-Pacheco, E. Flores, H. Hopfl, V. Barba, F.J. Fernandez, N. Cabirol, H.I. Beltran. *Inorg. Chem.*, **44**, 5370 (2005).
[38] N. Farfan, T. Mancilla, R. Santillan, A. Gutierrez, L.S. Zamudio-Rivera, H.I. Beltran. *J. Organomet. Chem.*, **689**, 3481 (2004).
[39] M.S. Refat, I.M. El-Deen, Z.M. Anwer, S. El-Ghol. *J. Mol. Struct.*, **920**, 149 (2009).
[40] R.V. Singh, P. Chaudhary, S. Chauhan, M. Swami. *Spectrochim. Acta, Part A*, **72**, 260 (2009).
[41] M.T. Kaczmarek, R. Jastrzab, E. Holderna-Kedzia, W. Radecka-Paryzek. *Inorg. Chim. Acta*, **362**, 3127 (2009).
[42] M.V. Angelusiu, S.-F. Barbuceanu, C. Draghici, G.L. Almajan. *Eur. J. Med. Chem.*, **45**, 2055 (2010).
[43] T.S.B. Baul. *Appl. Organomet. Chem.*, **22**, 195 (2008).
[44] G.G. Mohamed, M.M. Omar, A.A. Ibrahim. *Eur. J. Med. Chem.*, **44**, 4801 (2009).
[45] B. Rozycka-Roszak, H. Pruchnik, E. Kaminski.. *Appl. Organomet. Chem.*, **14**, 465 (2000).
[46] A. Olzynska, M. Przybylo, J. Gabrielska, Z. Trela, S. Przestalski, M. Langner. *Appl. Organomet. Chem.*, **19**, 1073 (2005).
[47] H.I. Beltran, C. Damian-Zea, S. Hernandez-Ortega, A. Nieto-Camacho, M.T. Ramírez-Apan. *J. Inorg. Biochem.*, **101**, 1070 (2007).